QUT Digital Repository:
http://eprints.qut.edu.au/

QUT

This is the submitted version of the following journal article:

Ke, Xuebin, Zheng, Zhan Feng, Liu, Hongwei, Zhu, Huai Yong, Gao, Xue Ping, Zhang, Li Xiong, Xu, Nan Ping, Wang, Huanting, Zhao, Hui Jun, Shi, Jeffrey, & Ratinac, Kyle R. (2008) High-flux ceramic membranes with a nanomesh of metal oxide nanofibers. *Journal of Physical Chemistry B*, *112*(16), pp. 5000-5006.

High-Flux Ceramic Membranes with a Nanomesh of Metal Oxide Nanofibers

Journal:	*The Journal of Physical Chemistry*
Manuscript ID:	jp-2007-09837r.R2
Manuscript Type:	Article
Date Submitted by the Author:	01-Feb-2008
Complete List of Authors:	Ke, Xuebin; Queensland University of Technology, School of Physical and Chemical Sciences Zheng, Zhanfeng; Queensland University of Technology, School of Physical and Chemical Sciences Liu, Hongwei; Queensland University of Technology, School of Physical and Chemical Sciences Zhu, Huai Yong; Queensland University of Technology, School of Physical and Chemical Sciences Gao, Xueping; Nankai University, Materials Chemistry Zhang, Lixiong; Nanjing University of Technology, State Key Laboratory of Materials-Oriented Chemical Engineering Xu, Nanping; Nanjing University of Technology, State Key Laboratory of Materials-Oriented Chemical Engineering Wang, Huanting; Monash University, Departments of Chemical Engineering Zhao, Huijun; Griffith University, Gold Coast Campus, School of Environmental and Applied Sciences Shi, Jeffrey; The University of Sydney, School of Chemical and Biomolecular Engineering Ratinac, Kyle; The University of Sydney, Electron Microscope Unit

scholarONE™
Manuscript Central

High-Flux Ceramic Membranes with a Nanomesh of Metal Oxide Nanofibers

Xue Bin Ke[1,2], Zhan Feng Zheng[1], Hong Wei Liu[1], Huai Yong Zhu[1], Xue Ping Gao[3], Li Xiong Zhang[2],

Nan Ping Xu[2], Huanting Wang[4], Hui Jun Zhao[5], Jeffrey Shi[6], Kyle R. Ratinac[7]

[1] School of Physical and Chemical Sciences, Queensland University of Technology, QLD 4001, Australia, Email: hy.zhu@qut.edu.au

[2] State Key Laboratory of Materials-Oriented Chemical Engineering, College of Chemistry and Chemical Engineering, Nanjing University of Technology, Nanjing 210009, China

[3] Institute of New Energy Material Chemistry, Department of Materials Chemistry, Nankai University, Tianjin 300071, China, Email: xpgao@nankai.edu.cn

[4] Departments of Chemical Engineering, Monash University, Clayton, VIC3800, Australia

[5] Australian Rivers Institute and The Griffith School of Environment, Gold Coast Campus, Griffith University, QLD 4222, Australia

[6] School of Chemical and Biomolecular Engineering, The University of Sydney, Sydney NSW 2006, Australia

[7] Electron Microscope Unit, The University of Sydney, Sydney NSW 2006, Australia

Abstract: Traditional ceramic separation membranes, which are fabricated by applying colloidal suspensions of metal hydroxides onto porous supports, tend to suffer from pin-holes and cracks that seriously affect the quality of the membranes. Other intrinsic problems for these membranes include dramatic losses of flux when the pore sizes are reduced to enhance selectivity, and dead-end pores that

make no contribution to filtration. In this work, we propose a new strategy to tackle these problems by constructing a hierarchically structured separation layer on a porous substrate using large titanate nanofibers and smaller boehmite nanofibers. The nanofibers are able to divide large voids into smaller ones without forming dead-end pores and with the minimum reduction of the total void volume. The separation layer of nanofibers has a porosity of over 70% of its volume, while the separation layer in conventional ceramic membranes has a porosity below 36% and inevitably includes dead-end pores that make no contribution to the flux. This radical change in membrane texture greatly enhances membrane performance. The resulting membranes were able to filter out 95.3% of 60-nm particles from a 0.01-wt% latex while maintaining a relative high flux of between 800 and 1000 L/m^2·h, under a low driving pressure (20 kPa). Such flow rates are orders of magnitude greater than those of conventional membranes with equal selectivity. Moreover, the flux was stable at approximately 800 L/m^2·h with selectivity of more than 95%, even after six repeated runs of filtration and calcination. Use of different supports, either porous glass or porous alumina, had no substantial effect on the performance of the membranes fabricated in this way; thus, it is possible to construct the membranes from a variety of supports without compromising functionality. The Darcy equation satisfactorily describes the correlation between the filtration flux and the structural parameters of the new membrane. The assembly of nanofiber meshes to combine high flux with excellent selectivity is an exciting new direction in membrane fabrication.

Keywords: ceramic membrane; nanofiber; flux; titanate; boehmite

Introduction

Porous ceramic membranes find application in many separation processes, including purification of water and air, enrichment of radioactive materials for nuclear energy, separations in the petrochemical, pharmaceutical and food industries, and in removal of contaminants.[1-2] Separation membranes of various metal oxides, including ZrO$_2$,[3] TiO$_2$,[4-6] SiO$_2$,[7,8] Al$_2$O$_3$[9,10] and their composites, have been prepared by sol-gel processes. These membranes were developed for filtration, for membrane reactors

and as functional materials. However, conventional ceramic membranes currently suffer from a serious loss of flux when pore sizes are reduced to improve their selectivity. This problem is intrinsically linked to the structure of the conventional membranes.[11,12] The colloidal suspensions are applied layer by layer in a sequence of decreasing particle sizes that reduces the size of the inter-particle voids to achieve better selectivity. The top-layers fabricated by this approaches are aggregates of particles, and are unable to combine a large flux with high selectivity (of filtering out small particles) because most of the volume of the separation layers is occupied by particles rather than by the voids that function as passageways. Consequently, the flux declines dramatically when pore sizes are reduced to increase selectivity. In addition, the conventional fabrication approach often suffers from formation of pin-holes and cracks during the drying and calcination processes.[13,14] These problems cause a high rate of defects and thus inflate the cost of the products.

To solve these problems, a radical change in membrane texture is necessary, particularly the texture of the separation layer that controls the performance of the resultant membrane in terms of flux and selectivity. It is well known that the mesh structure formed from threads or fibers represents the most efficient structure for pressure-driven membrane-filtration processes. Such structures are able to achieve high selectivity while maintain a high flux because the fibers divide large voids into smaller ones without forming dead-end pores and with the minimum reduction of the total void volume. The porosity in the separation layer of nanofibers can be over 70% of its volume. In contrast, the separation layer in conventional ceramic membranes has a porosity of below 36% and inevitably includes dead-end pores that make no contribution to the flux. Therefore, in principle, using fibril particles to construct separation layer is an effective approach for developing efficient filtration membranes. Recently thin, free-standing films have been synthesized by using extremely long and thin nanocomposite fibers, such as cadmium-hydroxide or copper-hydroxide nanostrands.[15-17] These nano-fibrous, free-standing films on a polycarbonate membrane filter showed clear size selectivity for proteins and double-stranded DNA, while retaining extremely high filtration rates. Moreover, they offer potential of novel applications by adding optical, biological, electrical and/or magnetic functionality.[17]

Recently, it has become possible to construct nanomesh membranes entirely from ceramic materials due to the ready availability of new ceramic nanofibers.[15-22] Membranes fabricated with ceramic fibers should inherit the advantages of conventional ceramic membranes, such as superior thermal and chemical stability and long operation life. In our previous communication,[14] ceramic nanofilters with a hierarchically structured separation layer were constructed on a porous α-alumina substrate by using large titanate (labeled "T") nanofibers and small boehmite (AlOOH) nanofibers. This approach was based on the latest developments in nanostructures of metal oxides. The resulting membranes, which incorporate layers of randomly oriented fibers (LROF), can effectively filter out species larger than 60 nm at flow rates orders of magnitude greater than conventional membranes, and are inherently free from structural deficiencies such as cracks, pin-holes dead-end pores and from severe sintering during membrane regeneration.

In the present study, separation layers are constructed from nanofibers of boehmite and titanate on porous glass supports, rather than the porous α-alumina supports used previously, thereby allowing comparison of membrane performance with different supports. We conduct a comprehensive study of the structural evolution of the separation layers formed through a controlled and repeated coating procedure and of the performance of the membranes during each stage of fabrication. This offers insights into the relationship between the filtration flux and the structural parameters of the membrane, as analyzed via the Darcy equation. Finally, we test the structural stability of the membranes and the reproducibility of their performance after repeated calcinations at high temperatures.

Experimental Methods General Information

Membrane Preparation. Analytical-grade NaOH, NaAlO$_2$, HNO$_3$, ethanol, and acetic acid (from Aldrich) were used in the synthesis. Titanate nanofibers and boehmite nanofibers were prepared according to standard methods.[18-22] Titanate nanofibers were synthesized by a hydrothermal reaction between a concentrated NaOH solution and TiOSO$_4$.[21] Boehmite nanofibers were prepared by a hydrothermal treatment of aluminum-hydrate precipitate.[18,19] The Membrane Science and Technology

Research Center of Nanjing University of Technology provided α-alumina supports with a diameter of 30 mm, thickness of 2 mm and mean pore size of 0.8 μm. Porous glass supports of equal size were purchased from Schott (Germany); these had a mean pore size of 2 μm.

The titanate nanofibers were dispersed into ethanol to form a 0.2 wt% suspension. This was sonicated with an ultrasonic finger (200 W) for 10 min to achieve a homogeneous dispersion, which was applied in thin layers to the porous substrate by means of a spin-coater. The porous substrate was mounted on the chuck of the spin-coat processor (WS-400B-6NPP-Lite, Laurell) and the coating was applied at a spinning velocity of 1000 r/min for 2 min. Approximately 0.5 mL of the titanate-fiber suspension was used for each coating. The coated discs were air dried at 393 K and then calcined by heating at 1 K/min to 773 K with a 4 h hold. This coating-drying-calcining process was repeated for each layer of nanofibers. The resultant membranes were labeled with Tn, where n was the number of coatings. The same approach was used for applying 3 layers of 0.2 wt% of boehmite nanofiber suspension to the titanate-nanofiber layers. The same drying and calcining schedule was used between each coating, and the calcinations converted the boehmite nanofibers into γ-alumina nanofibers. The resultant membranes were labeled "Al".

Membrane Performance. The pore-size distributions of the membranes were determined by the liquid-liquid displacement method.[23] Separation efficiency was assessed by filtering 30 mL of diluted latex suspension through the membranes under a vacuum of 20 kPa. Various elutes, including dispersions of polydisperse particles, have been used in other studies for testing membrane performance. Some even use solutions of macromolecules with different molecular weight (e.g., poly ethylene glycol, PEG, MW ranging from 2000 to 150,000) to test ultrafiltration membrane (pore size between 1-100 nm).[12] In this study, however, we used latex with particles of known sizes and small polydispersity to allow us to directly relate the filtration performance of the ceramic membrane to its underlying pore structure, which is a key parameter of the ceramic separation membrane. The suspensions contained 0.01 wt% of polymer spheres of known sizes, which were diluted from 10 wt % suspensions (Duke

Scientific Corporation). To calculate a mean flow rate, the time was recorded as each 5 mL of filtrate passed through the membrane.

Sample Characterization. The liquids were sampled before and after filtration for analysis by scanning electron microscopy (SEM) and UV-Vis spectroscopy.[24-26] The specimens for SEM were prepared by dropping 5 µL of solution on a cover glass, which was dried under vacuum and then gold coated (BioRad SC500 sputter coater). Images were taken with an FEI Quanta 200 and, for high-resolution images, a JEOL JSM 6400F field-emission SEM. The efficiency of membrane separation was estimated directly by comparing the numbers of latex spheres in images of the dried suspension and dried filtrate. To obtain a particle count, the number of latex spheres in a 2.7×2.1 µm area of an image was counted; for each sample, the counts in at least five different regions (images) were used to calculate a mean particle count per unit area. These means were then compared to determine separation efficiency. To confirm the results from SEM analysis, UV-visible spectroscopy (Cary100, Varian Inc.) also was used to analyze the particle concentrations before and after filtration.[26] Liquid specimen of 3 mL, which was a much large quantity than that of the SEM specimen, was for UV-visible measurement The intensity of the adsorption band at 205 nm was adopted to determine the concentration of the latex spheres by comparison with a calibration curve. The calibrated UV-Vis measurements gave similar results to the separation efficiency estimated from the SEM images, and so we will generally only present the latter data. The morphology of the nanofibers was recorded on a Philips CM200 transmission electron microscope (TEM) at an accelerating voltage of 200 kV. The nanofiber powders were deposited onto copper grids coated with holey carbon film.

Results and Discussion

The Construction of the LROF Structure. Figure 1 shows the LROF structures of the ceramic membranes and the morphology of the titanate and boehmite nanofibers. The boehmite nanofibers, which are converted to γ-alumina fibers when heated to temperatures above 723 K,[19, 20] and the titanate

nanofibers[21, 22] were used for making the LROF structures. From the TEM images, the titanate fibers are 50-100 nm in diameter and the small boehmite fibers are approximately 10 nm thick.

(Figure 1)

Figure 2 presents SEM images of a porous glass substrate, the titanate nanofibre coating on the substrate and the alumina-nanofiber coating on top of the titanate-nanofiber layer. The substrate consists of small (0.5 μm) and large (over 2 μm) silica (glass) particles (Figure 2a); at lower magnifications (not shown), the substrate surface is quite rough. From the manufacturer's data, the porosity of the substrate is approximately 30-40%. The key fabrication parameters for controlling the web-like structure of the spun nanofibres are the suspension loading, the spinning speed, and the drying process. As illustrated in Figure 2b, after three consecutive coatings with the titanate-nanofiber dispersion, the nanofibers lay down randomly on the substrate, covering the entire rough surface of the glass substrate and leaving no visible pin-holes or cracks. The coating parameters, such as fiber concentration and the number of coatings, can be optimized according to the nature of the porous substrate. Generally, a very rough substrate surface, as is the case for the porous glass, can be covered sufficiently by applying 3-5 coats of the 0.2 wt% dispersion. This eliminates the need for any intermediate-layer or for producing smooth substrate surfaces, which is a costly manufacturing prerequisite associated with fabrication of conventional membranes. Thus, the nanofibers can be applied directly to a variety of substrates and can also achieve significant cost efficiencies in membrane fabrication. More importantly, there are no pinholes, cracks or other defects after multiple nanofiber coatings and subsequent calcinations. This is vital for successful and cost-effective large-scale fabrication of nanomesh membranes and should see a marked reduction in rejects due to elmination of cracks and pinholes. Figure 2c is the top-view of a ceramic membrane with a hierarchical LROF structure, constructed using nanofibers of boehmite and titanate via the spin-coating approach.

(Figure 2)

Figure 3 displays the pore size distributions of the ceramic membranes in which the pore-diameter-distribution function, f(r), quantifies the fraction of the pores in a certain size range. The pore size of the glass substrate is up to several microns (curve a, Figure 3), and the LROF structure of titanate fibers mainly has pores between 100 and 200 nm (curve b, Figure 3). Given the 50-100 nm diameters of the titanate fibers, it is difficult to further reduce the pore size of the coating to much below 100 nm. Instead, a LROF structure with smaller pores is formed on the top of the titanate-fiber layer by coating with the thinner boehmite nanofibers, which are calcined to form γ-alumina nanofibers. By coating with the smaller γ-alumina nanofibers, one can reduce the sizes of the filtration pores to tens of nanometers (curve c in Figure 3) and enhance the selectivity of the membrane. In this combined membrane structure, the titanate nanofibers act as a scaffold to support the γ-alumina fibers.

(Figure 3)

Separation Performance of LROF structure. The filtration efficiency of the membranes was tested by filtering latex spheres out of aqueous dispersion. Figure 4 shows the SEM images of the dried suspensions and filtrates with different sizes of latex particles. By quantitatively comparing these images, we estimated the separation efficiency of the LROF structures. Complete removal (100% of retention) was achieved for the 200-nm spheres, approximately 98% retention of 108-nm spheres and more than 95% for 60-nm spheres. It also is evident from Figure 4 that the latex manufacturer's reported particle sizes represent only nominal values and that the spheres are not monodisperse in size, especially at the smaller diameters.

(Figure 4)

To achieve a better understanding of the functionality of the nanofiber layers, the filtration performance after each coating-drying-calcining cycle was tested with 0.01-wt% latex suspensions; the results are shown in Figure 5. After three coatings with titanate nanofibers, the LROF structure is capable of retaining 100% of the 200-nm latex spheres (Figure 5a) with a flow rate close to 2000 $L/m^2 \cdot h$, which is approximately 50% of the flux for the porous glass substrate. The first coating results in a large reduction in flux; however, the subsequent titanate-fiber coatings cause only slight decreases in flux while considerably improving membrane selectivity. This is a unique feature of the LROF structure.

(Figure 5)

The subsequent coatings of γ-alumina fibers on the top of titanate fibers cause a substantial decrease in the flux (Figures 5a and b). Nevertheless, the ability of the membrane to retain smaller particles is enhanced. The membrane with three coatings of γ-alumina fibers on the top of the coated titanate fiber layers was found to be capable of retaining 97.3% of the 108-nm spheres and 100% of the 200-nm spheres.

Figure 6 shows the separation performance of the membranes at various fabrication stages. The tests were carried out using a test sample of 0.01-wt% latex suspension with particle size of 60 nm. The measured flux of the final product membrane with randomly oriented titanate nanofibers and alumina nanofibers was about 950 $L/m^2 \cdot h$, with a high retention of 95.3% (Figure 6). The retention was calculated from both SEM images of the dried suspensions and filtrates and the UV-visible spectra of the suspensions and filtrates. As displayed in Figure 6b, the intensity of the adsorption band at 205 nm for the filtrate is only very low relative to that for the suspension, indicating a very low concentration of latex spheres in the filtrate.[26] The flow rate of the membrane is significantly greater than the typical fluxes (45 $L/m^2 \cdot h$) obtained from membranes prepared by conventional approaches[27] that exhibit similar selectivity performance under the pressure of 10 kPa. These results demonstrate an outstanding

characteristic of the LROF structured membranes; namely, that a high flux can be achieved without compromising the high selectivity.

(Figure 6)

It is apparent that the membranes with only one or two coatings of randomly oriented titanate nanofibers retain a higher flux, but have poor selectivity (Figure 6a). This probably is due to incomplete coverage by the fibers. Generally, complete coverage over the substrate surface can be achieved by three coatings, which gives a marked increase in selectivity accompanied by a decrease in flux.

The flux through the glass support is much larger than that of α-alumina support presented previously[14] due to its larger pore size. Although the flux for the porous glass substrate is greater than 4500 L/m^2·h, which is 3-4 times higher than obtained from the α-alumina substrate, a similar flux (between 800 and 1000 L/m^2·h) was obtained when filtering 60-nm latex spheres for the LROF membranes with either porous glass or α-alumina substrates. Thus, as expected, the flow rate is essentially independent of the substrate layer, when the LROF membranes were prepared with the same nanofibers by the same fabrication procedures. This is because the characteristics of the denser top-layer are the decisive factors for the flux and selectivity of the resultant membranes.

The high flux of the LROF structure can be attributed to its superior structural features including large pore volume, asymmetric cross-section structure with thin separation layer and absence of dead-end pores. For instance, filters made of stainless steel fibers with diameters ranging from 1 to 30 μm could only achieve porosities of between 65 and 85%.[28] Comparatively, a porosity of over 70% can be attained in an ideal mesh structure made of nanofibers with a thickness of 10 nm and a uniform pore size of 60 nm.[14] The porosity of a mesh structure does not vary substantially with the size of the fibers, and it is much higher than the porosity of randomly packed, monodisperse, spherical oxide particles in ceramic membranes, which is 36% or less.[29] The nanofibers in the LROF structure more effectively divide a specific volume into small voids and yet occupy a much smaller space compared with packed spherical

nanoparticles, thereby enabling the LROF structure to be much more efficient than the conventional top and intermediate layers of aggregated particles.[30,31] Moreover, there are no dead-end pores in the unwoven-mesh structure, so that all the pores between the fibers are interconnected and thus able to act as effective passages for fluid flow.

It is known that the flux of a pressure-driven membrane process can be described by the Darcy equation:[28]

$$Q = \frac{B \cdot A \cdot \Delta P}{\mu \cdot t}$$

For a given membrane system, the membrane area, A, and the fluid viscosity, μ, are fixed parameters. The transmembrane pressure difference, ΔP, is a controllable parameter, generally with a known value. Thus, the membrane flux, Q, depends only on the permeability factor, B, of the filter medium and the thickness, t, of the membrane. For fiber-based membranes, porosity is almost constant and B is determined by the Kozeny-Carman equation, which is proportional to the fiber diameter d_f^2.[28] So the permeability of a fibrous membrane, as estimated from the Darcy equation, should be proportional to d_f^2/t, which can be estimate by the flux ratio obtained from the membranes fabricated with three coatings of titanate fibers (i.e., T3 in Figure 6a), Q_{Ti}, and three coatings of γ-alumina nanofibers on the top of the titanate fibers (i.e., Al in Figure 6a), Q_{Al}. That is:

$$Q_{Ti}\Big/Q_{Al} = \frac{d_{Ti}^2 / t_{Ti}}{d_{Al}^2 / t_{Al}}$$

The mean thicknesses of the titanate nanofibers and the γ-alumina nanofibers were estimated by image analysis of the TEM results (the images in Figure 1 are the representatives of the images used for the analysis) as 60 and 10 nm, respectively. The mean thicknesses of the layers of titanate nanofibers and the layers of γ-alumina nanofibers in the LROF membranes were measured from SEM images of the cross section of the membrane. The thicknesses for the γ-alumina-fiber and titanate-fiber layers are approximately 0.5 μm and 7.5 μm, respectively. The ratio, Q_{Ti}/Q_{Al}, estimated from the experimental data and the Darcy equation was found to be 2.4. Fluxes of pure water passing through the two membranes

were measured, which are slightly higher than the fluxes shown in Figure 6a. The ratio derived from the water fluxes is approximately 2.1, in good agreement with the calculated result, suggesting the Darcy equation can be used to predict the performance of these new membranes.

Regeneration and thermal stability. Figure 7 shows the XRD patterns of the LROF structure. As expected, the porous glass substrate only shows a broad region of diffracted intensity between 15 and 30°, which is characteristics of the range of inter-atomic bond lengths in this amorphous material. The most intense diffraction peak of the titanate structure (labeled "T") is observed after the titanate nanofibers were applied onto the substrate. Finally, only the boehmite peaks can be seen (labeled "B") after coating by the boehmite fibers.

(Figure 7)

Calcination of the membranes after spin-coating creates strong bonds between the fibers and between fibers and the substrate, in addition to converting the boehmite nanofibers into γ-alumina. The titanate fibers are stable up to 973 K.[21,22] It is most likely that the surface hydroxyl groups on the fibers the substrate condense in the contacting areas. This releases water molecules and results in formation of direct bonds between the fibers themselves and between the fibers and the substrate so that the LROF structures are bonded together after calcination. Therefore, the membranes made of LROF structures should be mechanically and thermally stable during heating to high temperatures. This is an important merit for ceramic membranes because it allows us to conveniently clean or regenerate the used membranes by heating. Figure 8 shows the performance of a membrane with separation layers of titanate and alumina nanofibers after multiple regenerations by heating at 773K for 4 h. The separation properties were measured after each heating and are illustrated in the figure. The flux is stable at approximately 800 L/m^2·h with a selectivity of more than 95%.

(Figure 8)

For a conventional separation layers formed from compact ceramic particles, high-temperature heating inevitably results in particle sintering, which causes deterioration of selectivity and flow rate.[19] Sintering of particles commences from the contacting areas of particles. The contact areas between fibers are much smaller than those of particles of other low-aspect-ratio morphologies. Thus, there is no substantial sintering in the LROF structures of nanofibers during thermal regeneration. The small contact areas between fibers also reduce the risk of forming cracks during the drying or dehydration process. These are significant advantages of the LROF structures over the separation layers in conventional ceramic membranes.

Additional benefits of using titanate nanofibers are their high compatibility with biological substances because of their low-toxicity, their ability to withstand dissolution in water due to their low solubility, and their photostability.[32,33] Moreover, the alumina fibers have the ability to attract and retain electronegative particles such as viruses and bacteria because of the alkaline point of zero charge of alumina (approximately pH 9).[13] This widens the potential applications of the novel membranes to deal with separations involving biological substances.

Conclusion

This study clearly demonstrates that the separation efficiency of ceramic membranes can be improved significantly by constructing the separation layers with nanofibers. The mesh structure formed from fibers is the most efficient structure for filtration processes because fibers are able to divide large voids into smaller ones without forming dead-end pores and with the minimum reduction of the available void volume. The porosity in the separation layer of nanofibers is much larger than that of separation layer in conventional ceramic membranes. This explain why ceramic membranes with a hierarchical LROF structure as the separation layer exhibit a very high flux of between 800 and 1000 L/m^2·h, and a excellent selectivity of about 95.3 % for removal of 60 nm latex spheres.

Moreover, such a LROF structure has very low risk of forming cracks, pin-hole and dead-end pores or significant sintering, because it is constructed from fibers. To date, these sorts of problems and the low filtration flux have seriously limited the applications of ceramic membranes produced from small particles. Because there is much less sintering between nanofibers during repeated calcination, the performance of the membranes does not deteriorate obviously with thermal regeneration. The flux passing through the membrane is stable at approximately 800 L/m^2·h with the selectivity of more than 95% for removal of 60-nm latex sphere.

The LROF structure is also insensitive to the underlying porous support. The performance of the membranes constructed on porous glass substrates is similar that of membranes made on porous α-alumina supports, as long as the separation layers are prepared with the same nanofibers by the same procedure, which avoids placing any specific requirements on the porous support. We found that the relationship between the filtration flux and thickness of the separation layers of nanofibers can be described reasonably well by the Darcy equation, which is useful knowledge for designing new filtration processes to employ these efficient, new membranes.

The simplicity and flexibility of the raw materials and fabrication process mean that we are able to tailor the selectivity of the membranes by choosing fibers that meet the requirement of specific applications. The concept and the approach of constructing a hierarchical LROF structure as a separation layer provide new opportunities in developing the next generation of ceramic membranes with high flux. The fabrication of these membranes is relative straightforward and economical, compared with that of conventional ceramic membranes, and this approach can be scaled-up readily to fabricate ceramic membranes for practical applications.

References and Notes

(1)   Verweij, H. *J. Mater. Sci.* **2003**, 38, 4677-4695.

(2)   Cot, L.; Ayral, A.; Durand, J.; Guizard, C; Hovnanian, N.; Julbe, A. *Solid State Sci.* **2000**, 2, 313-334.

(3)   Gestel, T.V.; Kruidhof, H.; Blank, D.H.A.; Bouwmeester, H. J. M. *J. Membr. Sci.* **2006**, 284, 128-136.

(4)   Fuertes, M. C.; Soler-Illia, G. J. A. A. *Chem. Mater.* **2006**, 18(8), 2109-2117.

(5)   Sairam, M.; Patil, M. B.; Veerapur, R. S.; Patil, S. A.; Aminabhavi, T. M. *J. Membr. Sci.* **2006**, 281(1-2), 95-102.

(6)   Wu, C. H.; Huang, K. S.; Chern, J. M. *Ind. Eng. Chem. Res.* **2006**, 45(6), 2040-2045.

(7)   Yoo, S.; Ford, D. M.; Shantz, D. F. *Langmuir* **2006**, 22(4), 1839-1845.

(8)   de Vos, R. M.; Verweij, H. *Science* **1998**, 279, 1710-1711.

(9)   Uhlhorn, R. J. R.; Huisintveld, M. H. B. J.; Keizer, K.; Burggraaf, A.J.; *J. Mater. Sci.* **1992**, 27, 527-537.

(10)   Tang, K.; Yu, J.; Zhao, Y.; Liu, Y.; Wang, X.; Xu, R. *J. Mater. Chem.* **2006**, 16, 1741-1745.

(11)   Schäfer, A. I.; Fane, A. G.; Waite, T. D. *Nanofiltration-principles and applications*, Elsevier, Oxford, **2003**.

(12)   Bhave, R. R. *Inorganic Membranes: Synthesis, Characterisation and Applications,* New York, Van Norstrand Reinhold, **1991**.

(13)   Tepper, F.; Rivkin, T. *Filtr. Separat.* **2002**, 39, 16-19.

(14)   Ke, X. B.; Zhu, H. Y.; Gao, X. P.; Liu, J. W.; Zheng, Z. F. *Adv. Mater.* **2007**, 19, 785-790.

(15)   Ichinose, I.; Huang, J.; Luo, Y. *Nano. Lett.* **2005**, 5, 97-100.

(16)   Peng, X.; Jin, J.; Ichinose, I. *Adv. Func. Mater.* **2007**, 17, 1849-1855.

(17)   Peng, X.; Jin, J.; Ericsson, E. M.; Ichinose, I. *J. Am. Chem. Soc.* **2007**, 129, 8625-8633.

(18)   Shen, S. C.; Chen, Q.; Chow, P. S.; Tan, G. H.; Zeng, X. T.; Wang, Z.; Tan, R. B. H. *J. Phys. Chem. C* **2007**, 111, 700-707.

(19)   Zhu, H. Y.; Riches, J. D.; Barry, J. C. *Chem. Mater.* **2002**, 14, 2086-2093.

(20)   Zhu, H. Y.; Gao, X. P.; Song, D. Y.; Bai, Y. Q.; Ringer, S. P.; Gao, Z.; Xi, Y. X.; Martens, W.; Riches, J. D.; Frost, R. L. *J. Phys. Chem. B* **2004**, 108, 4245-4247.

(21)   Zhu, H. Y.; Gao, X. P.; Lan, Y.; Song, D. Y.; Xi, Y. X.; Zhao, J. C. *J. Am. Chem. Soc.* **2004**, 126, 8380-8381.

(22)   Zhu, H. Y.; Lan, Y.; Gao, X. P.; Ringer, S. P.; Zheng, Z. F.; Song, D. Y.; Zhao, J. C. *J. Am. Chem. Soc.* **2005**, 127, 6730-6736.

(23)   Calvo, J. I.; Bottino, A.; Capannelli, G.; Hernandez A. *J. Membr. Sci.* **2004**, 239, 189-197.

(24)   Kang, P. K.; Shah, D. O. *Langmuir* **1997**, 13, 1820-1826.

(25)   Akthakul, A.; Hoxhbaum, A. I.; Stellacci, F. A.; Mayes, M. *Adv. Mater.* **2005**, 17, 532-535.

(26)   Leiknes, T.; Ødegaard, H.; Myklebust, H. *J. Membr. Sci.* **2004**, 242, 47-55.

(27)   Yang, S. Y.; Ryu, I.; Kim, H. Y.; Kim, J. K.; Jang, S. K.; Russell, T. P. *Adv. Mater.* **2006**, 18, 709-712.

(28)   Vanhoutte, G. *NPT procestechnologie*, **2001**, 8, 25-27.

(29)   Guizard, C. G.; Julbe, A. C.; Ayral, A. *J. Mater. Chem.* **1999**, 9, 55-65.

(30)   Barhate, R. S.; Ramakrishna, S. *J. Membr. Sci.* **2007**, 296, 1-8.

(31)   Podgórski, A.; Balazy A.; Gradoń L. *Chem. Eng. Sci.* **2006**, 61, 6804-6815.

(32)   Linsebigler, A. L.; Lu, G.; Yates, J. T., Jr. *Chem. Rev.* **1995**, 95, 735-758.

(33)   Khan, S. U. M.; Al-Shahry, M.; Ingler, W. B. Jr. *Science* **2002**, 297, 2243-2245.

Figure 1 Schematic illustration of the layers in the ceramic membranes and TEM images of the boehmite (top) and titanate (bottom) nanofibers.

Figure 2. During construction of the nanomesh ceramic membranes on porous glass supports, the coatings are monitored by SEM. a) top-view of the porous glass substrate; b) after three coatings with 0.2-wt%-titanate suspension; c) after three coatings with 0.2-wt%-AlOOH suspension. Many of the rods observed in micrographs b and c are bundles of fibers rather than single fibers.

Figure 3 Pore-size distributions of the ceramic membranes. a) glass support; b) the membrane after three coatings of titanate fibers; c) the membrane after the subsequent three coatings of boehmite fibers.

Figure 4 SEM images of the latex dispersions and their filtrates. a) and b). the dispersion and filtrate of 200 nm latex spheres, respectively; c) and d) the dispersion and filtrate of 108 nm spheres, respectively; e) and f) the dispersion and filtrate of 60-nm spheres, respectively. The scale bars are 500 nm in length.

Figure 5 The filtration properties of the membranes during the course of fabrication, as tested with 0.01-wt% suspension of a) 200-nm latex spheres and b) 108-nm latex spheres. A different membrane was used to produce the data presented in each panel.

Figure 6 The performance of a membrane at the main stages of assembly when filtering a 0.01-wt% latex containing 60-nm spheres. a) filtration flux and selectivity; b) UV-vis absorption spectra of the suspension and filtrate from the filtration process Al in panel a); c) a top-view of a membrane with the LROF structure after the filtration Al in panel a, showing the 60-nm spheres.

Figure 7 XRD patterns of the LROF structure. a) glass substrate; b) the sample after three coatings of titanate (T) fibers on the glass substrate; c) the membrane obtained after three coatings with boehmite fiber (B) on the top of the titanate nanofibers.

Figure 8 Filtration performance of a membrane with LROF structure after each of six consecutive cycles of filtration and calcination. Performance was tested with 60-nm diameter particles.
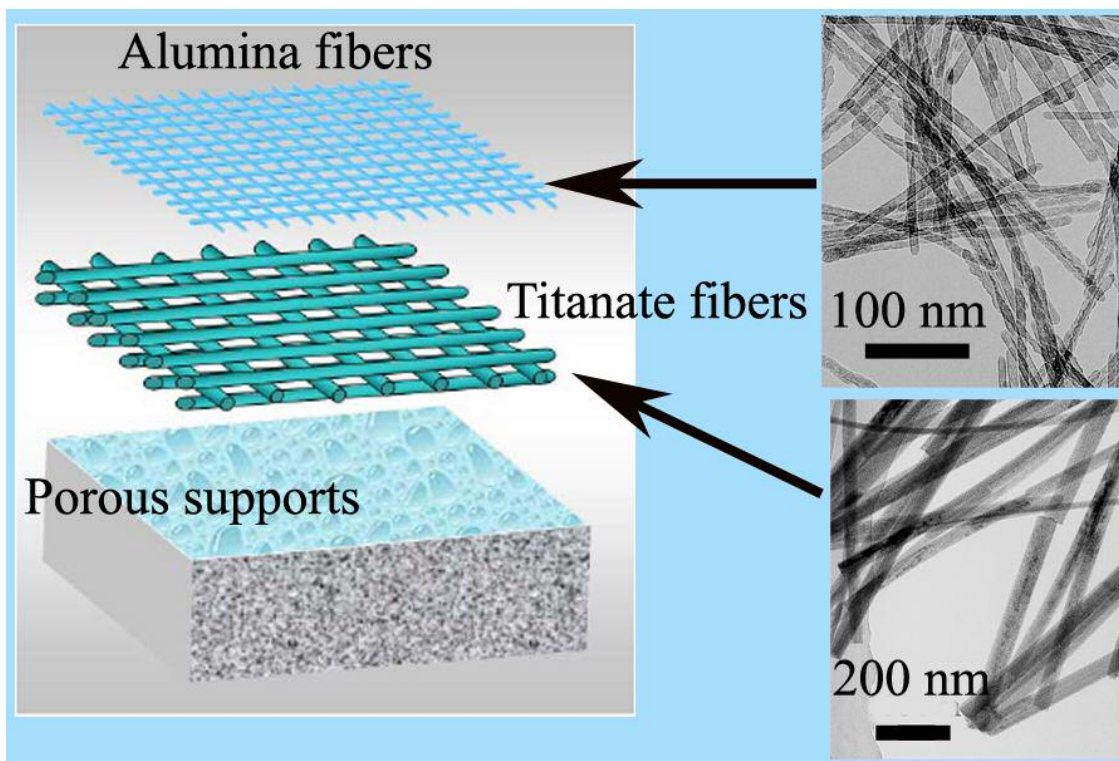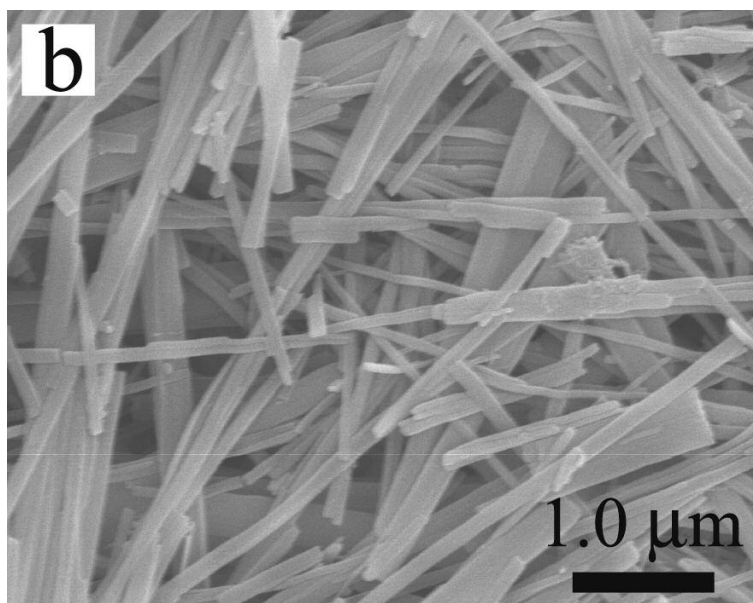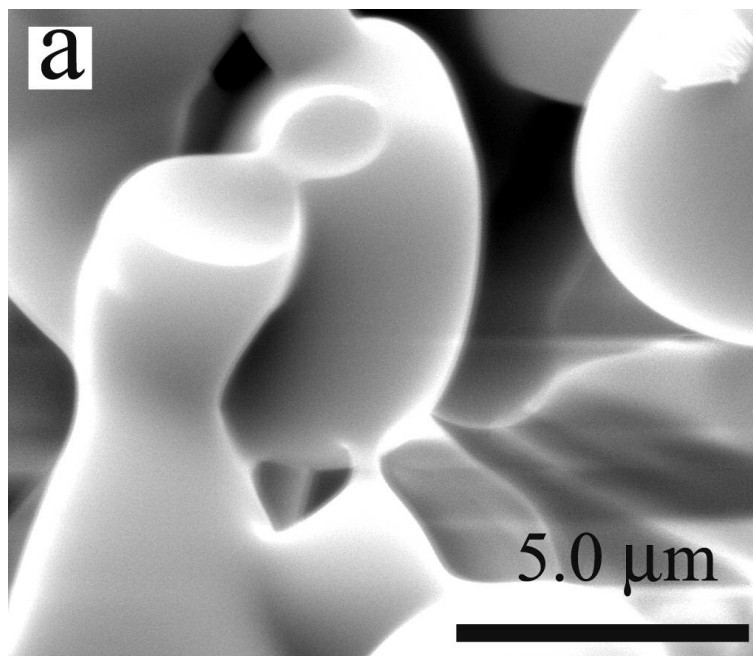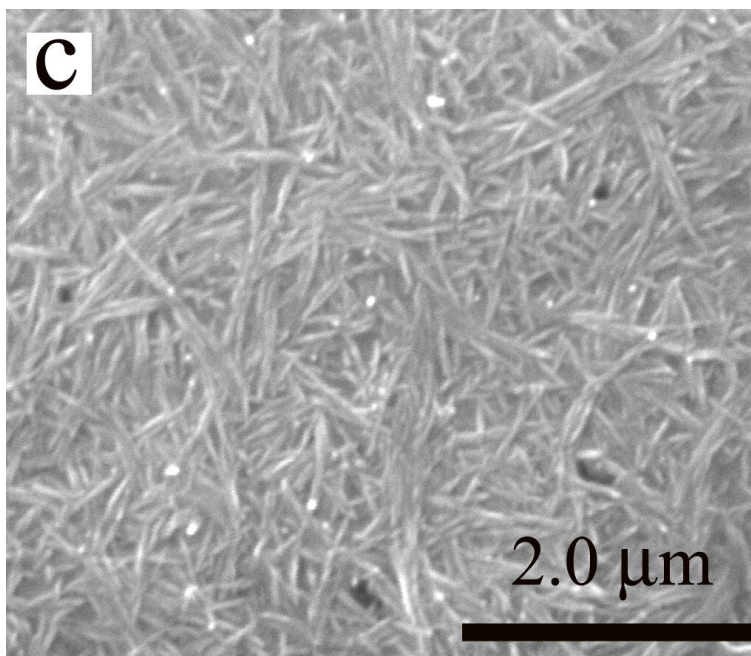
Figure 1

1
2
3
4
5
6
7
8
9
10
11
12
13
14
15
16
17
18
19
20
21
22
23
24
25
26
27
28
29
30
31
32
33
34
35
36
37
38
39
40
41
42
43
44
45
46
47
48
49
50
51
52
53
54
55
56
57
58
59
60
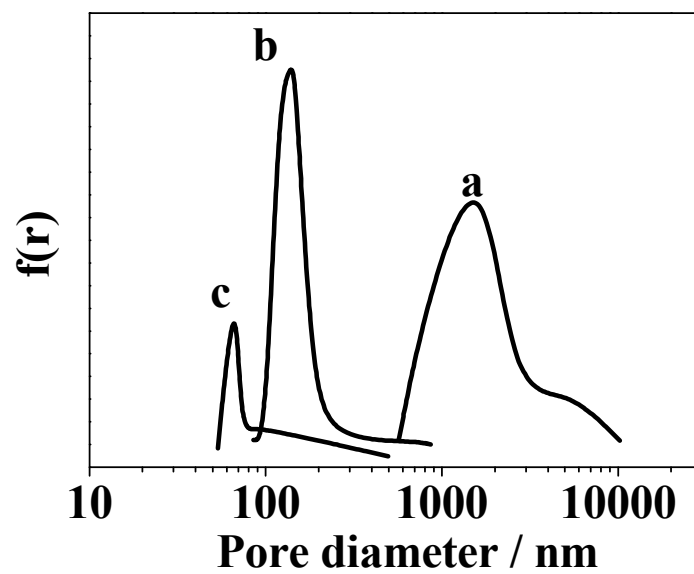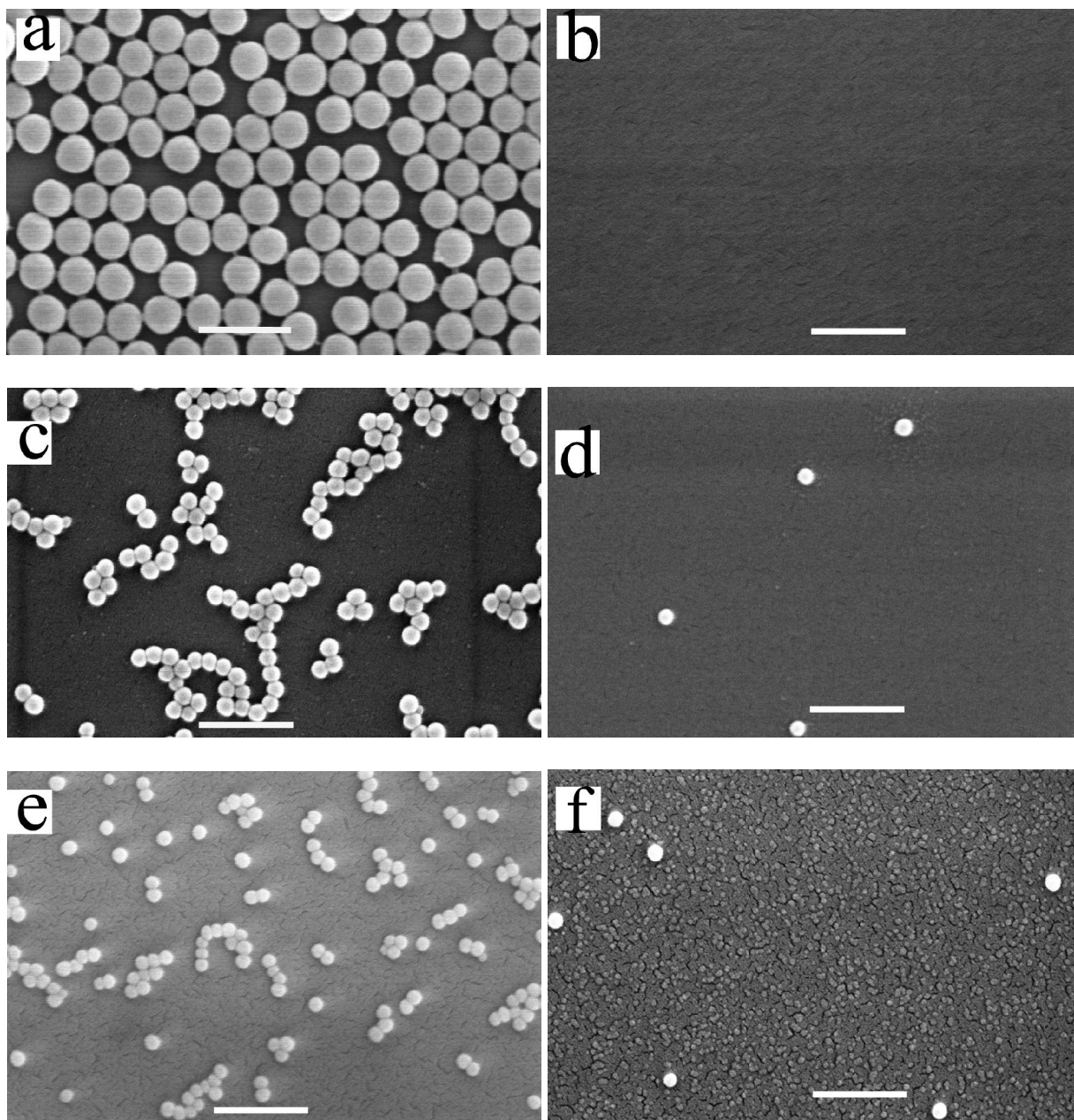
Figure 2

Figure 3

Figure 4
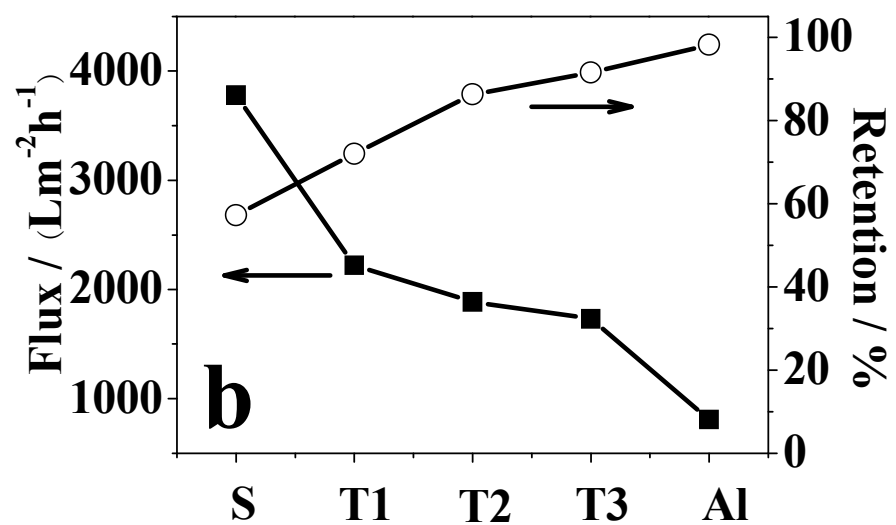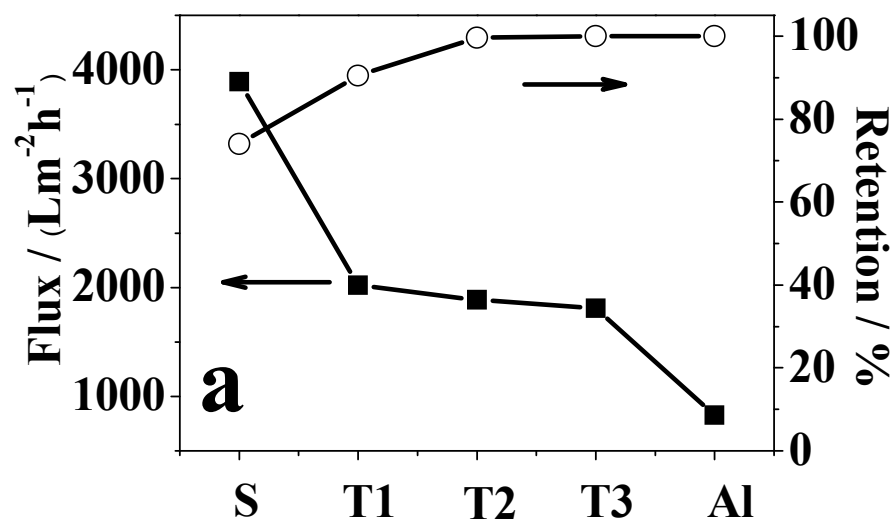
Figure 5
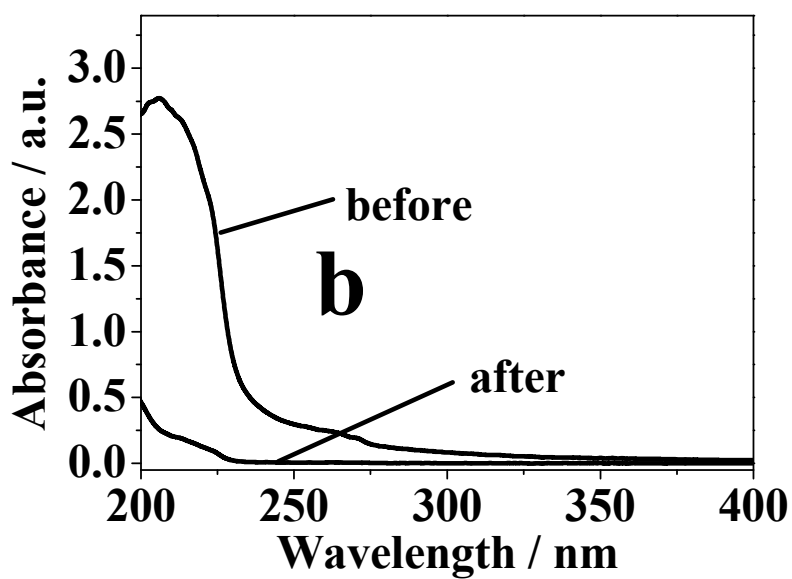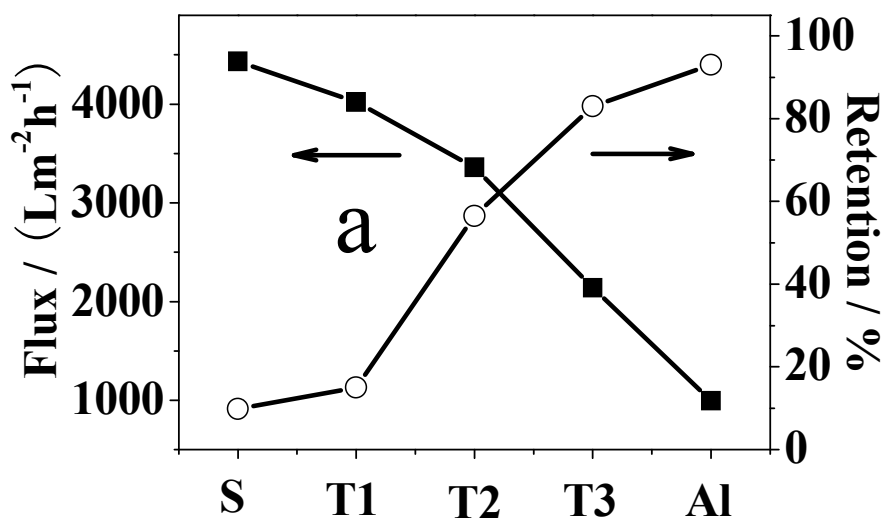
Figure 6

Figure 7

Figure 8